MINISTÉRIO DA CIÊNCIA E TECNOLOGIA
INSTITUTO NACIONAL DE PESQUISAS ESPACIAIS

IDENTIFICATION AND SENSOR FAILURE DETECTION ALGORITHMS APPLIED TO SPACE ROBOTIC JOINT

Adenilson Roberto da Silva*
Luiz Carlos Gadelha de Souza*
Bernd Schaefer+

INPE
São José dos Campos
2004

IDENTIFICATION AND SENSOR FAILURE DETECTION ALGORITHMS APPLIED TO SPACE ROBOTIC JOINT

Adenilson Roberto da Silva*
Luiz Carlos Gadelha de Souza*
Bernd Schaefer[+]
Instituto Nacional de Pesquisas Espaciais - INPE
Av. dos Astronautas,1758 – S J Campos, Brazil
[+]*German Aerospace Centers- DLR*
Institute of Robotics and Mechatronics
D82234 -Wessling
Adenilson.Silva@dss.inpe.br

ABSTRACT

The space environment imposes hard constraints in the design and control of robots because the dynamic behavior of the robot is quite different from its on-ground behavior. The modeling task becomes very complicated (or almost impossible) if one wants to take into account all the environmental conditions, which are present in the real environment. Therefore, in-flight dynamics data are required, with primary goals to update and validate mathematical models and gain confidence in the modeling process. Thus, the identification process is a very suitable choice to obtain a model with a high degree of fidelity. The failure detection task is very important in any engineering system. In space experiments, the knowledge of the sensor is almost crucial, because (normally) these experiments are very expensive. The loss of a sensor shall not jeopardize the whole experiment. In this paper, the robotic joint modeling and a integrated parameters identification – failure detection strategy is presented. The modeling process is carried out by using the Newtonian approach and the on-line identification is based in a modified version of RLS (Recursive Least Squares) algorithm. The analytical sensor failure detection uses the MOESP (Multi Output State Space Identification) algorithm as a baseline for the failure detection strategy. The developed strategy has been tested by using the real measurements taken from IRJ (Intelligent Robotic Joint) Experiment built at DLR Oberpfaffenhofen. Several tests have been performed which represent the situation where a single (and multiple) sensor failure is simulated and presented. In the tests, the integrated strategy has proved its desired performance, and it presented remarkable results in both: failure detection and on-line parameters identification.
Keywords: identification, modeling, failure detection, space robotics.

SYMBOLS

A = Matrix which represents the dynamics in the state space model

B = Matrix representing the actuator location in the state space model

C = Matrix representing the sensors location in the state space model

D = Matrix

J = Moment of inertia (Kg. m^2)

T = Torque (N. m)

T_d = Damping torque (N. m)

T_g = Gravity torque (N. m)

K_m = Motor constant (N. m/A)

N = Gear reduction

$\mathbf{x}$ = State vector

$\mathbf{y}$ = Output vector

vaf = Variance accounted for

Var = Variance

E = Expected value

$\mathbf{L}$ = Estimator gain

$\mathbf{P}$ = Estimator covariance matrix

Greek Symbols

$\Delta\theta$ = Relative position (input position – output position)

$\Delta\dot{\theta}$ = Relative velocity (input velocity – output velocity)

δ = Lower bound for errors

ε = Relative error between estimation and measurements

λ = Estimator forgetting factor

φ = Measurement matrix

θ = Angular position (rad)

$\dot{\theta}$ = Angular velocity (rad/s)

$\ddot{\theta}$ = Angular acceleration (rad/s^2)

Θ = Parameters vector

Subscripts

in relative to input side (motor side)

out relative to output side (link side of the joint

wg relative to wave generator of Harmonic Drive gear

fs relative to Flexspline of Harmonic Drive gear

$load$ relative to the load attached to the joint

$stiff$ relative to stiffness

INTRODUCTION

The failure detection (and isolation) in sensors and actuators is extremely relevant in systems engineering. Much effort in developing algorithms and strategies that efficiently detect and isolate failure in sensors has already been done (Basseville, 1997). Normally, two theories are applied: one using equipment redundancy and another using analytical redundancy. The equipment redundancy theory uses the information from two or more sensors to declare a failure of another one. The main characteristics of this theory are low computer effort and simple algorithms. These features result in heavy systems and are also more expensive (it is necessary to use redundant equipment). These characteristics sometimes make the failure detection process based on redundancy almost unfeasible. On the other hand, the failure detection based on analytical redundancy is attractive due to low costs (financial) and also from the design point of view.

Normally, these techniques are very complex and demand high computational efforts. Different methods have been applied to analytically detect and isolate sensor failure (Leohardt and Ayoulvi, 1997). The majority of these methods employ filtering techniques, Kalman filter for instance (Keller, 1999). The main problem to use these methods is the complexity and consequently, the high computational load. The heavy computational load appears because, normally, it is necessary to compute a bank of filters, which increase proportionally to the number of sensor to be monitored. In this paper, it is not intended to develop complex algorithms or sophisticated techniques, since the failure detection mechanism shall work in parallel with the parameters identification algorithm. Thus, the goal is to elaborate an algorithm that monitors the sensors output and also gives an alternative solution in case of failure. The technique presented further uses the subspace identification approach to derive the state space matrices, which are used in the failure detection algorithm.

The work is divided into three parts: the first part shows the mathematical representation of the IRJ experiment, the second shows the algorithm for failure detection and finally some results are presented.

MATHEMATICAL MODELING

The dynamics of the IRJ experiment can be represented by (Silva and Schäfer, 2001):

$$J_{in}\ddot{\theta}_{in} = T_m - T_{d\_in} - T_{wg} \tag{1}$$

$$J_{out}\ddot{\theta}_{out} = T_{fs} - T_{d\_out} - T_{d\_fscs} + T_{load} \tag{2}$$

Regarding the several torques acting on the joint, Eq. (1) and (2) are rewritten as

$$J_{in}\ddot{\theta}_{in} = K_m I_a - \left[T_{stiff}(\Delta\theta) + T_{d\_wg}(\Delta\dot{\theta}) \right] - T_{d\_in}(\theta_{in},\dot{\theta}_{in}) \tag{3}$$

$$J_{out}\ddot{\theta}_{out} = N \cdot \left[T_{stiff}(\Delta\theta) + T_{d\_wg}(\Delta\dot{\theta}) \right] - T_{d\_out}(\theta_{out},\dot{\theta}_{out}) - T_{d\_fscs}(\theta_{out},\dot{\theta}_{out}) + \hat{T}_g \sin\theta_{out} \tag{4}$$

The complete friction modeling and friction model can be found in (Silva, 2001).
Equations (3) and (4) are used as identification model. These two equations can be written a in regression form, which is useful to apply the RLS method:

$$\mathbf{y}(t) = \mathbf{\varphi}^T(t)\mathbf{\Theta} \tag{5}$$

where the damping and stiffness coefficients (grouped in vector $\mathbf{\Theta}$) are to be identified.

OUTPUT SENSORS ESTIMATION

The goal of the state space identification is to derive the set of state space matrices, which represent the relationship between input and output measurements (Silva, 2001):

$$\begin{aligned}\mathbf{x}(k+1) &= \mathbf{A}x(k) + \mathbf{B}u(k) \\ \mathbf{y}(k) &= \mathbf{C}x(k) + \mathbf{D}u(k)\end{aligned} \tag{6}$$

where $\mathbf{x}(k)$ are the states

   $\mathbf{u}(k)$ are the inputs, namely, $\theta_{motor}, \dot{\theta}_{motor}$ and $\ddot{\theta}_{motor}$

   $\mathbf{y}(k)$ are the output: θ_{out} and $\dot{\theta}_{out}$

   $\mathbf{A}, \mathbf{B}, \mathbf{C}$ and $\mathbf{D}$ are the unknown state space matrices to be determined.

Several methods (Juang and Pappa, 1985; Verhaegen and Dewilde, 1992, 1993) called Subspace Methods Identification (SMI) methods can be used to identify the unknown set of matrices. The algorithm MOESP has been selected due to its versatility and reliability and besides, this algorithm has already been successfully tested by DLR in the identification process of a helicopter using real data (Verhaegen et al, 1994).

STATE SPACE IDENTIFICATION ACCURACY CHECK

The state space matrices have been obtained by using all set of measurements available, namely, a set of 12 trajectories have been used. This procedure tries to ensure that the obtained set of matrices are able to deliver a satisfactory estimation even in the case when a different trajectory is used.

The estimation accuracy has been verified in a statistical way by using as an indicator the *vaf* (variance accounted for) that is represented by

$$vaf = \left(1 - \frac{\text{var}(y - \hat{y})}{\text{var}(y)}\right) * 100\% \tag{7}$$

where
$$\text{var}(x) = E\{[x - E(x)]^2\}$$
is the *x* variance. It is noted that when the value of *vaf* is high (close to 100), the better the estimation quality is. In case of the zero error, the *vaf* is 100 %.

FAILURE DETECTION ALGORITHM

Using the MOESP algorithm, it is possible to obtain a set of matrices that will estimate the states with a known degree of accuracy given the output of some sensors. For the case studied, the output of link position and velocity sensors are estimated given the information of input side (motor side).

It is important to note that the matrices given by Eq. (6) are obtained before any failure occurs, thus they are able to estimate all states with known statistical property.

The measurements to be monitored, θ_{out} and $\dot{\theta}_{out}$, are written in vector form (Silva, 2001)

$$\mathbf{y}(t) = \begin{bmatrix} \theta_{out} & \dot{\theta}_{out} \end{bmatrix} \tag{8}$$

The relative percental error between measurement and estimation is given by

$$\bar{\varepsilon}_e(t) = \left(\frac{\hat{y}(t) - y(t)}{\hat{y}(t)}\right) * 100\ \% \tag{9}$$

for $|\hat{\mathbf{y}}(t)| \geq \delta_{\min}$. Where $\delta_{\min}$ is the lower bound in the plant output.

When $\bar{\varepsilon}_e(t)$ is bigger than a specified value given by

$$\bar{\varepsilon}_{e_{\max}} = 100 + (\delta_e - vaf) \tag{10}$$

where *vaf* is given by Eq. (7) and δ_e is an estimation tolerance factor, and when a significant variation ($\bar{\varepsilon}_{io}(t)$) between motor sensor and link sensor occurs

$$\bar{\boldsymbol{\varepsilon}}_{io}(t) = \left(\frac{y_{in}(t) - y_{out}(t)}{y_{in}(t)} \right), \quad |y_{in}(t)| \geq \delta_{\min} \tag{11}$$

a failure in the respective sensor will be declared. After this instant, the sensor output is replaced by the estimation obtained from MOESP algorithm. If $\bar{\varepsilon}_e(t)$ has increased, but $\bar{\varepsilon}_{io}(t)$ lies in the acceptable range, a sensor failure cannot be declared. This means that the state space matrices are no longer valid. This situation can occur in cases where the system is experiencing large environmental changes, big temperature variations for instance. In this case, the *nominal* set of matrices shall be recalculated. This task is easily done by using the MOESP algorithm.

PHYSICAL PARAMETERS IDENTIFICATION

The recursive identification process is based on a modified version of RLS (Silva, 2001), which main steps are:

$$\mathbf{L}_k = \frac{P_{k-1}\phi_k}{\phi_k^T P_{k-1}\phi_k + \lambda}$$

$$\hat{\mathbf{\Theta}}_k = \hat{\Theta}_{k-1} + P_k\phi_k \left[y(k) - \phi_k^T \hat{\Theta}_{k-1} \right] \tag{12}$$

$$\mathbf{P}_k = \frac{1}{\lambda} \left(P_{k-1} - \frac{P_{k-1}\phi_k\phi_k^T P_{k-1}}{\phi_k^T P_{k-1}\phi_k + \lambda} \right)$$

where the forgetting factor (λ) is appropriately updated in order to improve the algorithm tracking.

ALGORITHMS TESTS AND RESULTS

Since all the necessary mathematical modeling has been derived, the next step is to verify the performance of the integrated process: failure detection and on-line identification. First, the ability of the failure detection strategy is verified by simulating a position sensor failure. After, the on-line identification is performed by using the outputs of the failure detection algorithm. If some measurements are declared failed, the correspondent sensor output is replaced by the MOESP estimation. It is important to note that the proposed strategy allows the identification algorithm to continue work and identifying the parameter related to failed sensor with a reasonable accuracy. The identification model used in the recursive identification is given by Eqs. (3) and (4). The main idea of the integrated process is represented in Fig. (1).
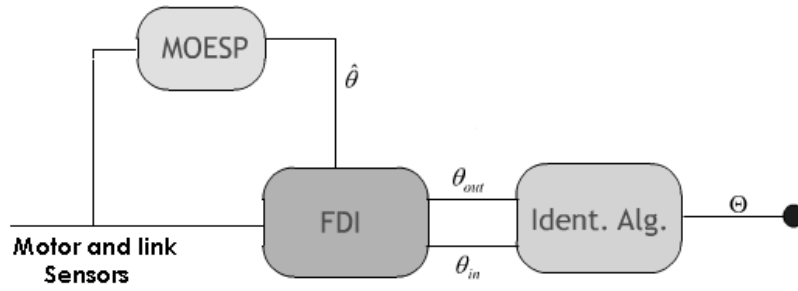
Figure 1 – FDI and Identification

STATE SPACE ESTIMATION ANALYSIS

The state space matrices have been estimated by using a set of 12 different trajectories. The data incorporate triangular trajectories as well as sinusoidal ones. In accordance with Eq. (6), the system to be identified is a MIMO one with three ($\theta_{motor}, \dot{\theta}_{motor}$ and $\ddot{\theta}_{motor}$) inputs and two outputs (θ_{out} and $\dot{\theta}_{out}$):

$$\mathbf{x}(k+1) = \mathbf{A_n}x(k) + \mathbf{B_n}u(k)$$
$$\mathbf{y}(k) \quad = \mathbf{C_n}x(k) + \mathbf{D_n}u(k)$$

(13)

The numerical values of the identified matrices are

$$\mathbf{A_n} = \begin{bmatrix} 0.9550 & -0.3232 \\ 0.0756 & 1.0041 \end{bmatrix}, \quad \mathbf{B_n} = \begin{bmatrix} -0.0277 & -0.9562 & -0.1894 \\ -0.0023 & -1.8935 & 0.4048 \end{bmatrix}$$

$$\mathbf{C_n} = \begin{bmatrix} 0.0058 & -0.0088 \\ -0.3263 & -0.4464 \end{bmatrix}, \quad \mathbf{D_n} = \begin{bmatrix} -0.0003 & 0.7962 & 0.0323 \\ 0.0068 & 5.3887 & -0.9836 \end{bmatrix}$$

where the index *n* means that the matrices have been obtained by using all type of trajectory available, thus corresponding to the *nominal* model. In order to illustrate the identification process, the inputs and outputs of MOESP algorithm are shown in Figs 2 and 3.
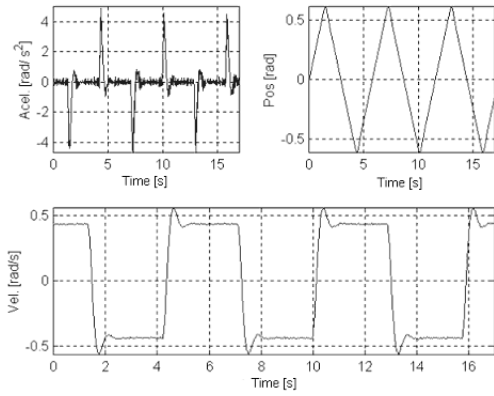
Figure 2 Inputs for MOESP algorithm - Triangular trajectory ($\dot{\theta}_{motor}$ = 25 rad/s)

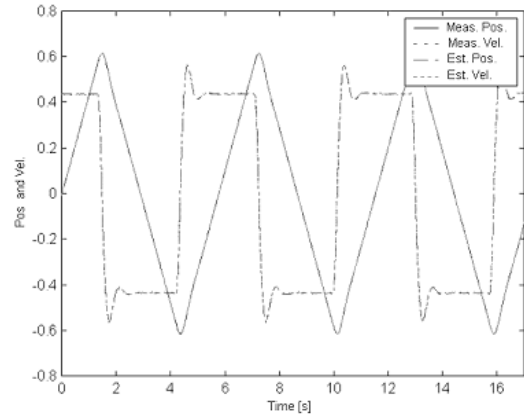Figure 3 Output measurements and respective estimate

Figure 3 shows the θ_{out}, $\dot{\theta}_{out}$ measured and its respective estimate $\hat{\theta}_{out}$ and $\dot{\hat{\theta}}_{out}$. In this figure, the two lines are almost indistinguishable, which shows the excellent result of the estimation process. This is confirmed by the *vaf* indicator

$$vaf_{pos} = 100\,\%, \qquad\qquad vaf_{vel} = 99.9898\,\% \qquad\qquad\qquad (14)$$

where vaf_{pos} is related to the position and vaf_{vel} is related to the angular velocity.

FAILURE SIMULATION

The failure detection mechanism described above has been tested by simulating different cases and situations. The cases differ due to the trajectories used and the situations due to the instant of failure: simultaneously or not.

Figure 4 shows the simulation of position sensor failure by using a triangular trajectory. The sensor has presented a failure at instant t= 5s, but the velocity sensor did not present a failure. The failure is simulated by replacing the real data by a random noise. It can be noted that the algorithm instantaneously detects the bad measurements delivered by the position sensor and replaces it by the corresponding estimation (Fig. 5). Because of the good accuracy, it is almost impossible to note the transition from real data to estimated one only by inspecting the plots.

The failure in the velocity sensor is detected in the same manner, namely, when the algorithm detects a variation in $\bar{\varepsilon}_e(t)$, a failure is declared. The measurement is replaced by the estimation and an estimated signal is available for the parameters identification algorithm.
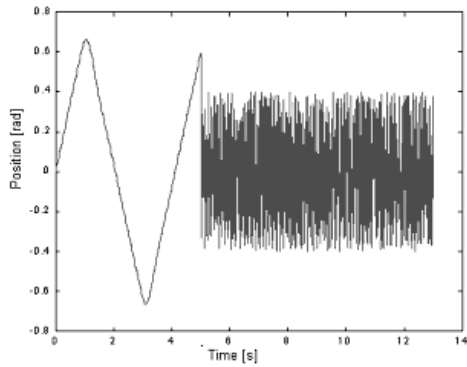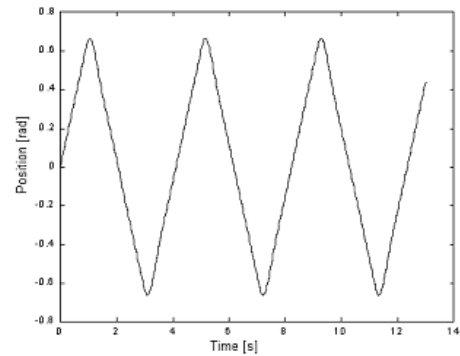
Figure 4 Sensor position failure

Figure 5 Link position after measurement reconfiguration

ALTERNATIVES UNDER FAILURES SITUATIONS

The identification techniques require not only a minimal number of measurements but also that these measurements are of good quality. In specific cases the IRJ experiment, may operate also in space environment. This fact shows that a special attention to the sensors and actuators shall be dispensed. Thus, several strategies and alternatives have been developed in order to investigate the special requirement for this task. An important detail to be considered is related to failure in sensors. Thus, aiming to maximize the available experiment information in case of failure occurrence, two solutions were found:

- Algorithm reconfiguration;
- Stiffness isolation.

It is important to note that the solutions proposed always try to maintain the low computer effort and also to keep the algorithm reconfiguration ability. The first requirement is needed because there exists the possibility to have on-board processing; normally the on-board computer has limited characteristics if compared to computers used on ground. The second requirement is needed because there is a high possibility of the system present time variant behavior. Therefore, the main requirements for the algorithm and strategy developed are: adaptation capability, reconfiguration and low computer effort.

SENSORS FAILURE SIMULATION

In the following, the parameters obtained by using identification algorithm under link velocity sensor failure (simulated) are presented. In the detection, isolation and estimation process, the procedure described above has been used. The model used is described by Eqs. (3) and (4), namely, the model incorporates the non-linear terms and cyclic errors.

The failure in the link velocity sensor is programmed to occur at t = 20s, and the corresponding measurement signal has been replaced by random noise (0,0.1). From this instant, the information given by this sensor is replaced by the MOESP estimation.

The behavior of the identification process by using MOESP estimation is shown in Fig. 6. It is observed that the accuracy given by the *vaf* indicator is confirmed. No oscillations have been observed after replacing the measured data by the estimated ones. The dashed lines in Figs. 6-9 represent the values obtained by the off-line identification using only measured data. It can be noted that the identification algorithm converges to the expected value using estimated state. This ensures that mission success is guaranteed even in the case of link velocity sensor failure. In Fig. 7 the stiffness and damping parameters are also shown. It can be noted that all parameters are very close to those obtained by off-line identification, showing that the estimation given by MOESP algorithm has no big effect in the global identification process.

In Fig. 8 and 9 the identification results are shown in the case where the MOESP estimation has been used. Considering the severe requirements (measurements of magnitude 10^{-9}) for stiffness parameters, one can conclude that the results are excellent. The parameters present small changes in comparison with the values obtained by off-line estimation using only measured data. The variations in the parameters range from 0.5 % (additional spring) to 10.5 % (term related to the Stribeck effect (Olsson, 1996)). The variation in $|T_N|\varpi_2^{-1}$ is justified by the high sensitivity of this term (This has been observed in the singular value analysis). Once, the identification process is reconfigured, and considering that the estimation is very good, there exists still a difference between measured and estimated ones. This difference is naturally reflected more sensitively in the parameters.
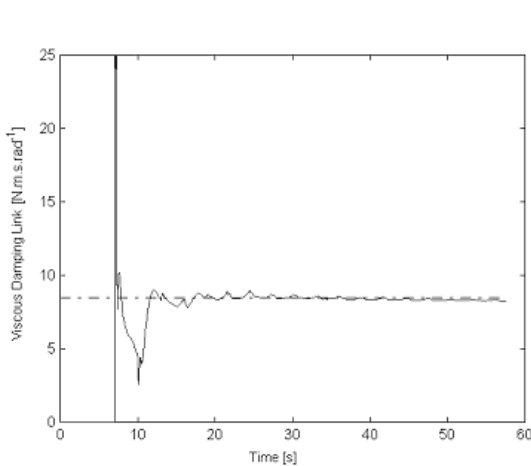

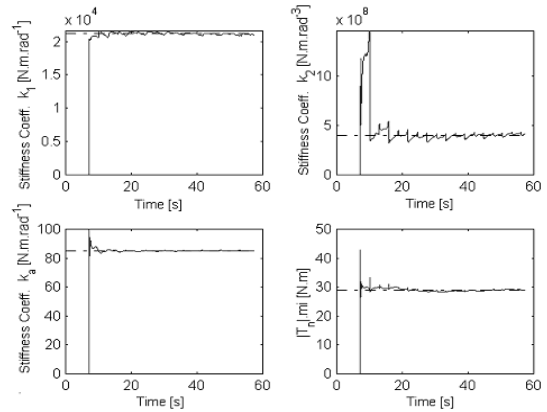Figure 6 Viscous damping identification (link) by using MOESP estimation

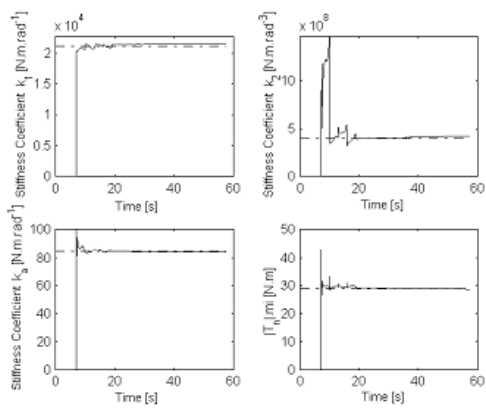Figure 7 Linear parameters – Using link velocity given by MOESP algorithm.

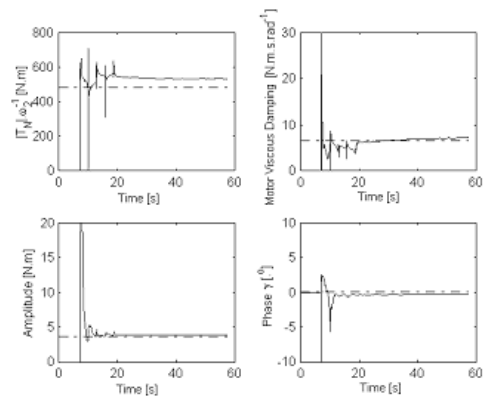Figure 8 Linear parameters – Using link position estimated by MOESP algorithm

Figure 9 Damping coefficients– Using link position estimated by MOESP algorithm

CONCLUSIONS

In this work, an algorithm for both failure detection and parameters identification has been developed. The developed algorithms have been applied and tested to identify dynamic parameters of IRJ experiment. The failure detection and isolation procedure has presented very low computer effort compared to the conventional procedures.

The integrated process (identification and failure isolation) shows efficiency in the failure detection and isolation of the data under failure suspect. Due to critical conditions of dynamic identification of stiffness coefficients, it can be concluded that the results obtained in the identification process by using MOESP estimates are remarkable, allowing immediately applications, such as adaptive control design.

REFERENCES

BASSEVILLE, M. Information Criteria for Residual Generation and Fault Detection and Isolation. **Automatica**. Vol 33, n° 5, pp. 783 – 803, 1997

JUANG, J. N.; PAPPA R. S. "*An Eigensystem Realization Algorithm for modal Parameter Identification and Model Reduction.* " – **Journal of Guidance, Control, and Dynamics.** v.8, n.5, Set-Oct, pp. 620-627, 1985.

KELLER, J. Y. Fault isolation Filter Design for Linear Stochastic Systems. **Automatica**. Vol 35, pp. 1701 – 1706, 1999

LEOHARDT, S. and AYOULVI, M. Methods of Fault Diagnosis. **Control Engineering Practice**. Vol 5 n° 5, pp. 683 – 692, 1997

OLSSON, H. Control Systems with Friction. PhD Thesis of **Lund Institute of technology**. Sweden. p. 172, 1996

SILVA, A. R and SCHÄFER, B. Harmonic Drive Modeling and Physical Parameters Identifications for Robotic Joints**. IX Diname – International Symposium on Dynamics Problems of Mechanics**. Mar. 2001 – Florianópolis, Brazil.

SILVA, A. R. Identificação de Parâmetros e Detecção de Falhas Aplicada a Manipuladores Espaciais, **INPE – Instituto Nacional de Pesquisas Espaciais,** Phd Thesis, 2001, 195pp.

VERHAEGEN, M. , VARGA, A. and GRÜBEL, G. Some Experience with MOESP Class of Subspace Model Identification Methods in Identifying the B) 105 Helicopter- **DLR Oberpfaffenhofen**, 1994, 26 pp

VERHAEGEN, M. and DEWILDE, P. Subspace Model Identification Part 2: Analysis of Elementary Output-Error State-Space Model Identification Algorithm. **International Journal of Control,** 1992 – Vol 36, N. 5, pp 1211-1241

VERHAEGEN, M. and DEWILDE, P. Subspace Model Identification Part 3: Analysis of Ordinary Output-Error State-Space Model Identification Algorithm. **International Journal of Control,** 1993 – Vol 58, N. 5, pp 555-586